Selective targeting of radiation-resistant tumor-initiating cells

Mei Zhang[a], Rachel L. Atkinson[a,b], and Jeffrey M. Rosen[a,1]

[a]Department of Molecular and Cellular Biology and [b]Graduate Program in Translational Biology and Molecular Medicine, Baylor College of Medicine, Houston, TX 77030-3498

Edited by George F. Vande Woude, Van Andel Research Institute, Grand Rapids, MI, and approved December 16, 2009 (received for review September 8, 2009)

Tumor-initiating cells (TICs) have been shown both experimentally and clinically to be resistant to radiation and chemotherapy, potentially resulting in residual disease that can lead to recurrence. In this study, we demonstrate that TICs isolated from p53 null mouse mammary tumors repair DNA damage following in vivo ionizing radiation more efficiently than the bulk of the tumor cells. Down-regulation of phosphatase and tensin homolog deleted on chromosome 10 (PTEN) was observed both in fluorescence activated cell sorting (FACS)-isolated TICs as compared to non-TICs and in TIC-enriched mammospheres as compared to primary tumor cells depleted of TICs. This effect was accompanied by increased Akt signaling, as well as by the direct activation of the canonical Wnt/β-catenin signaling pathway specifically within the TIC subpopulation by phosphorylation of β-catenin on serine 552. Using limiting dilution transplantation performed on p53 null tumor cells transduced with Wnt reporter lentivirus, we demonstrated that FACS sorting of cells expressing TOP-eGFP resulted in a marked enrichment for TICs. Furthermore, FACS analysis demonstrated that cells with active Wnt signaling overlapped with the TIC subpopulation characterized previously using cell surface markers. Finally, pharmacological inhibition of the Akt pathway in both mammospheres and syngeneic mice bearing tumors was shown to inhibit canonical Wnt signaling as well as the repair of DNA damage selectively in TICs, sensitizing them to ionizing radiation treatment. Thus, these results suggest that pretreatment with Akt inhibitors before ionizing radiation treatment may be of potential therapeutic benefit to patients.

Akt and Wnt signaling | DNA damage repair | p53 mouse model

A growing body of evidence has suggested that many cancers, including hematopoietic and solid tumors, may be driven by a small subpopulation of tumor-initiating cells (TICs, or cancer stem cells, CSCs). TICs can be isolated by fluorescence-activated cell sorting (FACS) using specific cell surface and other markers from the bulk of the tumor cells (1). Despite the recent improvement in overall mortality, many breast cancer patients fail to respond to conventional treatment, leading to tumor recurrence. One explanation for treatment failure may be the intrinsic resistance of TICs to radiation/chemotherapy. Clinical studies supporting this hypothesis have suggested that the TIC subpopulation is enriched in breast cancer patients following treatment with neoadjuvant chemotherapy (2). Targeting critical pathways that are specific to TIC function in combination with conventional therapies may be crucial for improved treatment of cancer.

The Wnt signaling pathway is well known for its roles in embryogenesis and cancer, as well as in cell fate determination in many normal tissues, including the mammary gland. Deregulated Wnt signaling has been reported in both mouse mammary tumors and human breast cancers (3). The central player of the canonical Wnt pathway is β-catenin, which, after translocating to the nucleus, transactivates a number of transcriptional targets (4). The Wnt signaling pathway plays a critical role in hematopoietic stem cell (HSC) self-renewal and differentiation to give rise to all lineages of the blood. Overexpression of activated β-catenin expands the pool of HSCs, whereas inhibition of the Wnt signaling pathway results in growth inhibition of HSCs (5). Phosphatase and tensin homolog deleted on chromosome 10 (PTEN) also plays an important role in regulating the self-renewal and proliferation of HSCs and neural stem cells (6, 7). Deletion of PTEN leads to activation of the PI3K/Akt pathway, whose prognostic significance has been reported in human breast cancers (8). Loss of PTEN, and thus the activation of the PI3K/Akt signaling pathway, contributes to chemoresistance in lung (9) and breast cancer (10). Enrichment of the stem/progenitor cell population has been reported in mouse models of human prostate and breast cancer following PTEN deletion, suggesting the important role of PTEN in self-renewal and tumor initiation (11, 12). PTEN loss has been shown to mediate resistance of TICs to chemotherapy (13), but the impact on radiation resistance remains to be examined.

To identify TICs, we employed previously a p53 null mammary tumor model in which tumors develop stochastically following transplantation of p53 null mammary epithelial cells into the cleared mammary fat pad of wild-type p53 syngeneic BALB/c mice. Whereas Lineage $(Lin)^{-}CD44^{+}CD24^{-/low}$ phenotype was identified as the cell surface marker for human breast cancers, we discovered in a panel of p53 null mammary tumors that the TIC subpopulation was highly enriched in $Lin^{-}CD29^{High}CD24^{High}$ ($Lin^{-}CD29^{H}CD24^{H}$), using the cell surface markers CD29 and CD24, previously employed to isolate normal mouse mammary stem cells (14, 15). Microarray analysis revealed increased expression of cell cycle checkpoint and DNA damage repair genes within the TIC subpopulation, suggesting that the TICs might be intrinsically more resistant to DNA damage induced by ionizing radiation (IR) and chemotherapy. In the present study, we determined that, although the initial responses to DNA damage were similar for the TICs and bulk tumor cells derived from these p53 tumors, the TICs exhibited more efficient DNA damage repair. The selective activation of the Akt and canonical Wnt signaling pathways within the tumorigenic TICs was demonstrated by the increased expression of phospho (p)-Akt and increased phosphorylation of β-catenin on serine (Ser) 552. Inhibition of the Akt pathway directly inhibited canonical Wnt pathway activation and selectively sensitized TICs to IR treatment.

Results

Tumorigenic Subpopulations with Stem Cell Properties. Concerns over the strategies used to identify TICs have led investigators to question if the experimental conditions and the lack of an appropriate microenvironment in xenograft models using immunocompromised mice have resulted in an underestimate of the frequency of TICs (16). To avoid these complications, we used a transplantable p53 null mouse mammary tumor model and lim-

Author contributions: M.Z. and J.M.R. designed research; M.Z. and R.L.A. performed research; M.Z., R.L.A., and J.M.R. analyzed data; and M.Z. and J.M.R. wrote the paper.

The authors declare no conflict of interest.

This article is a PNAS Direct Submission.

[1]To whom correspondence should be addressed. E-mail: jrosen@bcm.tmc.edu.

This article contains supporting information online at www.pnas.org/cgi/content/full/0910179107/DCSupplemental.

iting dilution transplantation experiments into the cleared mammary fat pad of syngeneic BALB/c mice to demonstrate that the $Lin^-CD29^HCD24^H$ subpopulation, representing overall ≈3–15% of the total cell population, displayed significantly increased tumorigenic potential as compared to other subpopulations, $Lin^-CD29^HCD24^{Low(L)}$, $Lin^-CD29^LCD24^H$, or $Lin^-CD29^LCD24^L$ (14). Using improved FACS sorting techniques, we now are able to reduce the number of cells required to form tumors to as few as 10 cells, which represents a TIC frequency of ≈1/27 and a 65-fold enrichment over the unfractionated population (Table 1). This frequency is >10-fold higher than reported previously (14), thus illustrating the absolute TIC frequencies are highly dependent on the experimental conditions employed. Although the calculated frequencies of TICs may, therefore, vary depending on the methods employed to isolate and transplant these cells, the fold enrichment observed between the TICs and the bulk tumor population was quite similar. For the following purposes, four independent tumors from the p53 null model were studied. Tumor T1 is a heavily keratinizing squamous adenocarcinoma, T2 is a well-differentiated papillary adenocarcinoma, T6 is an undifferentiated solid adenocarcinoma, and T7 is a solid adenocarcinoma of the usual undifferentiated type.

Tumorigenic $Lin^-CD29^HCD24^H$ Cells Are Radioresistant Due in Part to Increased DNA Damage Repair. Our previous studies demonstrated an ~10-fold increase in intrinsic radioresistance of TIC-enriched mammosphere cultures as compared to the total bulk tumor cells depleted of TICs cultured on a plastic substratum (14). To determine if this difference in the apparent DNA damage repair response was also observed in tumors exposed to IR-induced DNA damage in vivo, p53 null tumors were transplanted into the cleared fat pads of syngeneic BALB/c mice and allowed to grow to ≈1 cm in diameter. They were then exposed to a single dose of 6 Gy irradiation and individual subpopulations were isolated by FACS immediately following IR as well as 48 h later. FACS-sorted TIC and non-TIC populations were immunostained with antibodies directed against the γ-H2AX as well as 53BP1, cellular markers of DNA double-strand break formation (17), and the number of cells with foci was quantified to determine the response of the various tumor subpopulations to DNA damage. All four lineage negative subpopulations, $CD29^HCD24^H$ (TIC), $CD29^HCD24^L$, $CD29^LCD24^H$, and $CD29^LCD24^L$, displayed a similar number of cells exhibiting DNA damage foci immediately following radiation (Fig. 1 *A* and *B*), suggesting that there were not intrinsic differences in DNA damage caused by 6 Gy of IR. However, among the four subpopulations, only the TICs showed a dramatic difference in response to DNA damage 48 h later, with only 20% of the TICs containing γ-H2AX and 53BP1 foci as compared with ~70–80% of the other cell subpopulations (Fig. 1 *A* and *B*). These data suggest that a more efficient DNA damage checkpoint and repair mechanism may exist in TICs as compared to the other subpopulations. MTS cell proliferation assays performed on FACS sorted cells suggested that there were no differences in proliferation among these subpopulations (Fig. S1). Using a genetically engineered MMTV-Wnt-1 mouse model, Diehn et al. suggested that CSCs contain a lower level of reactive oxygen species (ROS) than the bulk of tumor cells, which might contribute to their radioresistance (18). To test if ROS also plays a role in the p53 null mammary tumor model, we employed MitoSOX and DCF-DA assays, which are highly selective detection methods for mitochondrial superoxide and intracellular concentrations of prooxidants, respectively. Under our experimental conditions with 6 Gy of IR, no significant differences were detected among the TICs vs. bulk tumor cells (Fig. S2).

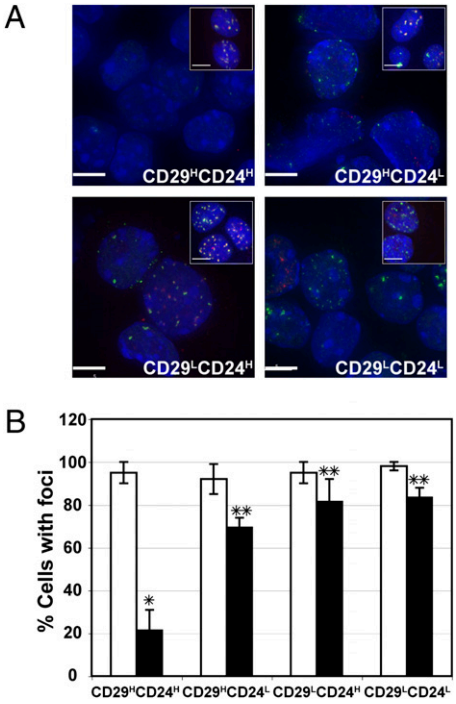

Fig. 1. Altered DNA damage repair in TICs. (*A*) γ-H2AX and 53BP1 foci of individual subpopulations isolated by FACS immediately following IR (*Insets*, ≈5 h posttreatment) and isolated by FACS 48 h later (≈53 h posttreatment). γ-H2AX, red; 53BP1, green; and DAPI, blue. (Scale bar, 5 μm.) (*B*) Similar numbers of cells exhibit DNA damage following 6 Gy (□, ≈5 h posttreatment), whereas DNA damage was significantly reduced 48 h later (■, ≈53 h posttreatment) in TICs as compared to the majority of tumor cells (*, $P < 0.03$; **, $P = 0.05$). Two hundred to ~500 cells from each subpopulation of cells were counted. Tumors T1, T6, and T7 were included in the study.

Activation of the PI3K/PTEN/Akt and Wnt Signaling Pathway in the TIC Subpopulation. A direct correlation between Akt activation, the repair of DNA damage, and radioresistance has been reported

Table 1. TICs were enriched in the $Lin^-CD29^HCD24^H$ subpopulation using improved cell isolation and FACS sorting techniques

Cells injected	5,000	1,500	1,000	100	50	25	10	TIC frequency (95% CI)
$Lin^-CD29^HCD24^H$		4/4	2/2	12/12	12/12	4/12	3/12	1/27 (1/42–1/18)*
$Lin^-CD29^HCD24^L$		2/4	4/6	4/12	2/12	0/8	0/6	1/786 (1/1,522–1/406)
$Lin^-CD29^LCD24^H$	4/6	2/8	2/7	0/8	0/6	0/2	0/6	1/4,470 (1/2,192–1/9,114 1/9,144–1/2,192)
$Lin^-CD29^LCD24^L$	2/6	2/8	0/7	0/8	0/6	0/2	0/6	1/10,822 (1/29,040–1/4,033)
Lin^-	2/3	6/10	4/9	2/12	1/10	0/4		1/1,749 (1/3,100–1/986)

Tumors T1 and T7 were freshly digested and individual tumor cells were FACS sorted as described in ref. 14 with the following modifications: shorter tumor digestion time of 1.5–2 h and larger nozzle size of 100 and 130 μm for FACS sorting. A BD four-laser FACSAriaII (Becton, Dickinson) was used, instead of the previous triple laser MoFlo (Cytomation).
*$P < 0.001$.

CELL BIOLOGY

previously using glioblastoma cell lines (19). Quantitative PCR (qPCR) analysis showed that the expression of *Pten* was decreased in TICs vs. all of the other cell types ($P < 0.01$) (Fig. 2*A*). As shown in Fig. S3, TICs were also larger in size than the other subpopulations, possibly as a reflection of alterations in *Pten* expression (*Discussion*). Therefore, to investigate the PTEN/Akt pathway directly, Western blot analysis was performed on freshly isolated TICs and non-TICs, as well as in mammospheres (MSs), which are enriched for TICs, as compared to total tumor cells depleting TICs (14). The levels of p-AKT^{Ser473} and AKT were tested directly between TICs vs. non-TICs, which displayed increased levels of active AKT in the TIC subpopulation (Fig. 2*B*). The PTEN/Akt signaling pathway was also activated in TIC-enriched MSs as shown by decreased expression of PTEN, and the increased expression of p-AKT and an indirect downstream target, p-mTOR^{Ser2448}, whereas total AKT and mTOR remained unchanged (Fig. 2*B*). Akt may directly regulate canonical Wnt signaling through phosphorylation of β-catenin on Ser552, thus increasing the nuclear translocation of β-catenin (20), and activation of canonical Wnt target genes, such as survivin. We observed increased expression of β-catenin^{Ser552} and survivin in freshly isolated TICs and MSs enriched for TICs, suggesting activation of the canonical Wnt pathway exclusively in the TIC subpopulation (Fig. 2*B*).

Characterization of the Canonical Wnt Pathway Using Lentiviral Transduction into Primary p53 Null Tumor Cells. Significant evidence has suggested that the Wnt/β-catenin pathway is highly implicated in uncontrolled self-renewal of cancer cells and radiation resistance during treatment (21, 22). This result led us to hypothesize that TICs might be characterized by increased canonical Wnt signaling. To test this postulate, we employed a lentivirus containing a TOP-eGFP pathway reporter to evaluate the importance of canonical Wnt signaling in the TIC subpopulation in several independent p53 null mammary tumors. Dissociated mammary tumor cells were transduced in suspension with the TOP-eGFP lentivirus, and cells were then transplanted into the cleared mammary fat pad of 3-week-old recipient mice to generate

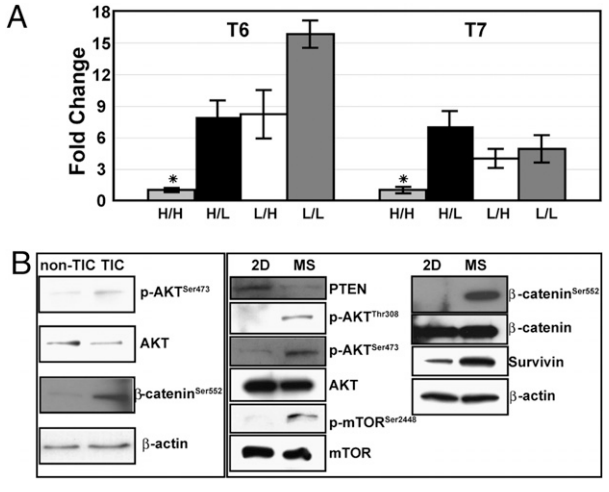

Fig. 2. Akt and Wnt signaling pathways were activated in TICs. (*A*) qPCR analysis of PTEN, using tumors T6 and T7. The relative expression of TIC was designated as "1" to calculate the fold change. Three biological replicates were included in each sample (*, $P < 0.01$). ■, Lin$^-$CD29^{H}CD24^H; ■, Lin$^-$CD29^{H}CD24^L; □, Lin$^-$CD29^{L}CD24^H; ■, Lin$^-$CD29^{L}CD24^L. (*B*) Western blot demonstrates activation of AKT and increased p-β-catenin^{Ser552}, a direct target of Akt activation, in freshly FACS isolated TICs, as well as in MSs enriched for TICs, as compared to non-TICs and the total tumor cells cultured on plastic (2D), which are depleted in TICs, respectively.

tumors. The frequency of the TOP-eGFP-positive cells detected by FACS varied among the different tumors studied from 2 to 7% (Fig. 3*A*). FACS analysis also demonstrated a marked overlap (90%) of the eGFP-positive cells with the TIC population characterized previously as CD29^{H}CD24^H in tumor T1 (Fig. 3*B*). Likewise, 70–75% of eGFP-positive cells were CD29^{H}CD24^H in tumor T6. Limiting dilution transplantation of eGFP-positive and -negative cells was performed as summarized in Table 2 with as few as 10 eGFP-positive cells giving rise to tumors. Interestingly, no tumors have been observed to date with 100 transplanted eGFP-negative cells. eGFP-positive cells derived from tumor T1 showed a 70-fold enrichment in TIC frequency, as compared to eGFP-negative cells, and a 20-fold enrichment in tumor T6.

Inhibition of Akt Signaling Reduces Mammary Stem Cell Self-Renewal in Vitro and Sensitizes Resistant MSs to IR Treatment. We next investigated if the treatment of MSs with the Akt inhibitor, perifosine, would inhibit the self-renewal of the TIC subpopulation and sensitize them to IR treatment. MSs treated with perifosine (20 μM) displayed reduced expression of p-Akt and p-β-catenin^{Ser552} as compared to the vehicle control (Fig. 4*A*), whereas total Akt and β-catenin remained unchanged. In addition, secondary MS formation was quantified following IR or perifosine treatment alone and the combination of perifosine plus IR treatment. A slight increase in MS forming efficiency was observed after IR treatment, whereas perifosine alone and perifosine together with IR markedly decreased the self-renewal ability of the TICs ($P < 0.03$) (Fig. 4*B*). These results indicate that Akt inhibition significantly reduced MS self-renewal potential, as well as sensitized them to IR treatment.

Perifosine Treatment Reduces the Proportion of TICs in the p53 Null Mammary Tumors and Sensitizes TICs to Radiation Treatment. We next determined whether similar effects would be observed in tumors treated in vivo and if this response to radiation and perifosine was related to effects on the repair of DNA damage. Accordingly, we compared the effects of perifosine with IR treatment in vivo, both in combination and individually. Mice were treated daily with 25 mg/kg of perifosine by oral gavage (perifosine only) or with PBS (untreated control) for 10 days. For IR treatment, mice were given a single dose of 6 Gy IR following 10 days of perifosine (perifosine + IR) or PBS (IR only) treatment. Forty-eight hours after the treatment, tumor cells were isolated and analyzed by FACS to determine the percentage of eGFP-positive cells in TOP-eGFP-transduced T1 tumors. The TICs from tumors T6 and T7 were analyzed by FACS using the cell surface markers CD29/CD24 as described previously (14). Limiting dilution transplantation experiments were then performed to determine the TIC frequency from each treatment group as compared with the control group.

As shown in Fig. 4*C* and Fig. S4, in all three independent tumors, radiation alone resulted in a significantly increased percentage of TICs, demonstrating that the TICs were more radiation resistant. Animals from tumors T1 and T7 irradiated at 2 Gy every 16 h for 2 days showed a similar enrichment of TICs to that observed with a single dose of 6 Gy (Fig. S5). In contrast, perifosine treatment alone decreased the percentage of T7 TICs by ~25% as compared to untreated tumors and by ~40% as compared to IR alone. Similarly, perifosine treatment alone reduced the number of TICs assessed by FACS by ~50% as compared to IR alone in tumors T1 and T6. Most strikingly, the combination of perifosine plus IR, however, showed a marked decrease by ~55–70% as compared to IR alone in TICs in all three tumors analyzed. Limiting dilution experiments using freshly digested, but unsorted tumor cells were performed to determine if the functional TIC frequencies correlated with the results obtained by FACS analysis. Accordingly, an increased TIC frequency was observed in the IR group, whereas perifosine treatment alone and perifosine plus IR treatment both resulted in a lower TIC frequency (Table 3),

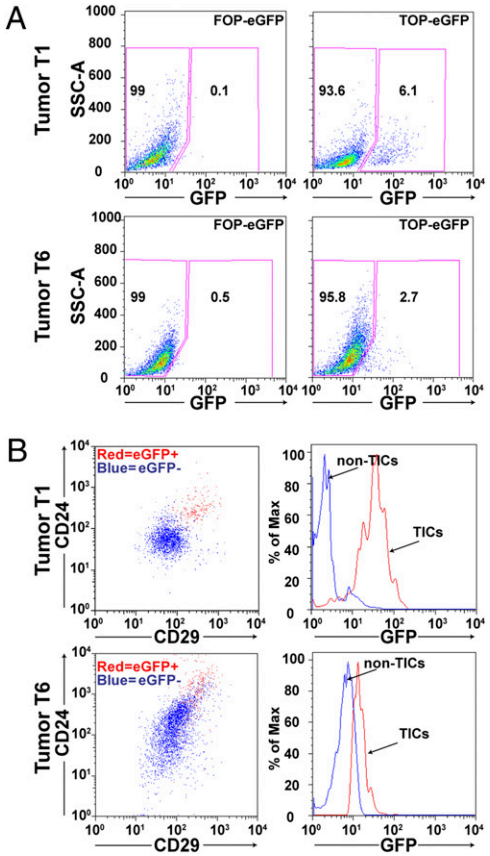

Fig. 3. Canonical Wnt signaling marks TICs in the p53 null mammary tumors. (*A*) Totals of 6.1% (T1) and 2.7% (T6) of tumor cells show GFP expression following transduction with lentiviral TOP-eGFP compared to little to no expression in the FOP-eGFP-transduced control. (*B*) FACS analysis shows that the majority (90% in T1 and 70–75% in T6) of eGFP-positive cells are also $CD29^{H}CD24^{H}$ (*Left*) and reciprocally most $CD29^{H}CD24^{H}$cells are also eGFP positive (*Right*).

consistent with the decreased percentage of the TICs observed by FACS analysis. In TOP-eGFP transduced T1 tumors, a 10-fold increase of TIC frequency was observed in the IR-treated group as compared with the nontreated control, whereas a 3- and a 4-fold decrease was seen in the perifosine- and the perifosine plus IR-treated groups, respectively. In tumor T7, the TIC frequency increased 2-fold in the IR-treated tumors, whereas it decreased 2-fold in the perifosine-treated group and 4-fold in the perifosine plus IR-treated group as compared with the control.

Finally, to test whether the effects of perifosine and IR on TIC frequency correlated with alterations in the DNA damage response of TICs, tumor cells from the perifosine plus IR group were FACS sorted, cytospun, and stained with antibodies against γ-H2AX and 53BP1. In striking contrast to the differences in DNA damage foci observed 48 h following irradiation in untreated TICs as compared to the other three subpopulations (Fig. 1), all four subpopulations now exhibited a similar level of DNA damage foci, suggesting that the repair of DNA damage in TICs was blocked by treatment with perifosine (Fig. 4*D*). Interestingly, there were no apparent differences in the other three subpopulations detected following perifosine treatment, supporting the observation that the DNA damage repair in TICs is uniquely dependent on the Akt/Wnt-β-catenin signaling pathway.

Table 2. TOP-eGFP positive cells enrich for TICs

Cells injected (T1)	1,000	500	100	10	TIC frequency (95% CI)
TOP-eGFP positive	4/4	6/6	3/5	4/6	1/48 (1/126–1/18)*
TOP-eGFP negative	1/4	1/6	0/5	0/6	1/3,389 (1/13,558–1/847)
Cells injected (T6)	1,000	500	100	10	TIC frequency (95% CI)
TOP-eGFP positive	6/6	4/6	4/6	1/6	1/225 (1/462–1/109)*
TOP-eGFP negative	1/6	1/6	0/6	0/6	1/4,443 (1/17,834–1/1,107)

Tumors T1 and T6 were transfected with the Wnt reporter TOP-eGFP and its control FOP-eGFP as described in *Materials and Methods*. The resulting tumors were collected and digested as described in *Materials and Methods* under *Preparation of Single Mammary Tumor Cells* and *Flow Cytometry*. TOP-eGFP-positive and -negative cells were isolated and transplanted into 3-week-old recipient mice.
*$P < 0.001$.

Discussion

Despite successful radiation and/or chemotherapy in many patients, some of the cells in the unique subpopulation of intrinsically therapy-resistant TICs, perhaps by virtue of their increased survival mechanisms, may reinitiate tumor growth following treatment. Tumors that recur are often associated with radioresistance with evidence suggesting that breast cancer stem/progenitor cells are enriched after radiation, because those cells are particularly resistant to radiation (23). Studies using both an immortalized mouse mammary epithelial cell line (Comma-D) and a human breast cancer cell line (MCF-7) demonstrated that stem/progenitor cells were more resistant to radiation as compared with the bulk of these cells (22, 24). More effective therapies will thus require the selective targeting of this crucial cell population.

In the p53 null mammary tumor model, TIC frequency was markedly enriched as compared to the bulk tumor cells (65-fold), allowing us to define the mechanisms responsible for TIC resistance to DNA damage and to investigate the pathways regulating this response. Our results and those of others have demonstrated that the resistance of TICs to radiation and chemotherapy is correlated with alterations in DNA damage repair. Following radiation, DNA damage checkpoint proteins were activated to a greater extent in glioma $CD133^{+}$ cells, brain tumor cells with TIC properties, than in $CD133^{-}$ tumor cells, suggesting that such TICs are responsible for tumor recurrence following radiation therapy (25). A key player in the Akt pathway, PTEN, was down-regulated in the TIC subpopulation, which subsequently led to the activation of this pathway. Cells isolated from the brains of *Pten* knockout mice as well as neurospheres derived from *Pten* deficient mice were larger in size than their respective controls (6). Gene expression analysis from cultured neurospheres of both *Pten* mutant and wild type showed a significant number of identified genes (248) up-regulated in *Pten* mutant neurosphers (6). Among them, 48 genes (19%) were also present in our TIC differentially up-regulated gene list. Consistently, TICs from p53 null tumors, with decreased expression of *Pten*, were larger in size than other cells (Fig. S3), suggesting that down-regulation of *Pten* in TICs may regulate cell size through a similar mechanism.

Because increasing evidence supports the radiation and chemotherapy resistance of TICs, we studied the effects of perifosine on inhibiting DNA damage repair to sensitize resistant TICs to IR treatment. Perifosine is an oral, anticancer agent that modulates the Akt signal transduction pathway and is used in the treatment of patients with multiple myeloma and metastatic colon cancer. Radiation sensitization of human bladder cancer cell xenografts has been reported after targeting the PI3K pathway in vivo (26). However, conflicting results have been reported as to the inhibition of the PTEN/PI3K/Akt signaling pathway and radiosensitization in brain tumors (27–29). The PTEN/Akt/β-catenin signaling pathway regulates mammary stem/progenitor self-renewal through the phosphorylation of GSK3β as reported recently by Wicha and colleagues (12). In their studies, perifosine was able to block pathway activation and reduce the tumor growth in breast tumor xenografts. To mimic the delivery method used in patients, we used oral gavage to

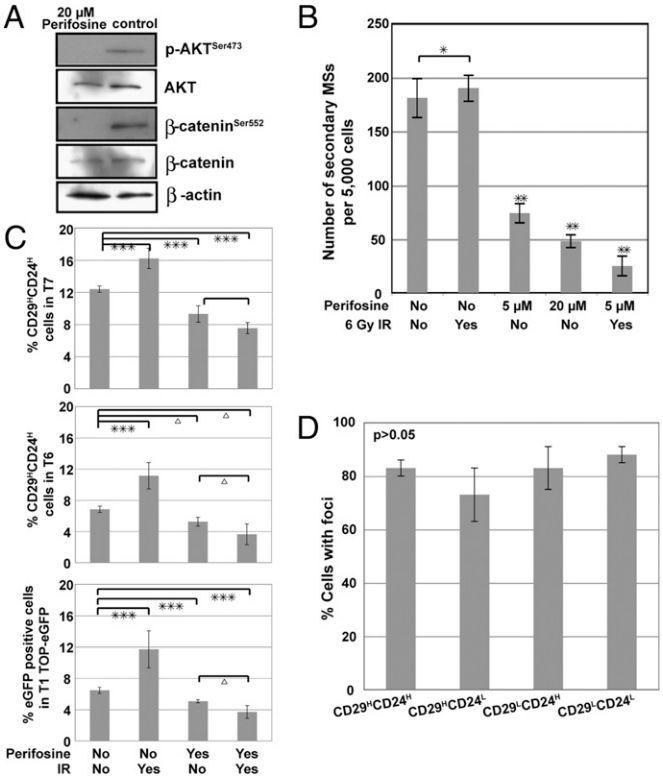

Fig. 4. Akt inhibitor perifosine-sensitized radiation-resistant mammary tumorspheres enriched for TICs in vitro as well as in vivo. (*A*) Western blot showing decreased active β-catenin and active Akt during perifosine treatment of MSs enriched for TICs. Proteins were isolated from perifosine-treated secondary MSs from T1. (*B*) Treatment of secondary MSs with perifosine inhibited their self-renewal and sensitized them to IR treatment (*, $P < 0.03$; **, $P < 0.01$) from tumors T1 and T7. Three replicates from each tumor were included. (*C*) Perifosine alone and perifosine plus 6 Gy IR treatment reduce the percentage of the TICs as shown by FACS analysis using tumor T7, tumor T6, and TOP-eGFP-transduced tumor T1. Five independent tumors from both untreated and IR alone groups were included for each tumor type. Ten tumors were included for perifosine alone and perifosine plus IR groups for each tumor type (***, $P < 0.002$; Δ $P < 0.05$). (*D*) A similar level of DNA damage foci observed from various subpopulations isolated by FACS 48 h following irradiation (≈53 h posttreatment) in perifosine plus IR treated groups. After perifosine plus IR treatment and FACS sorting, cells were cytospun and stained for DNA damage foci. Fifty to ~170 cells of each subpopulation were counted, and the percentage of cells with γ-H2AX or 53BP1 foci was calculated for each subpopulation. Tumors T1 and T7 were included in the study, and three replicates from each tumor were included. No significant differences were observed between TICs and the three subpopulations of cells ($P > 0.05$).

administer the drug. Importantly, our studies show that Akt activation can also result in direct phosphorylation and activation of β-catenin at Ser552, which may complement its known effects on the phosphorylation and inhibition of GSK3β. Thus, combinatorial effects of Akt activation are most likely responsible for the increased expression of downstream targets of the canonical Wnt/β-catenin pathway, such as survivin. Inhibition of Akt by perifosine treatment not only reduced the expression of p-Akt and β-catenin^{Ser552}, but also significantly reduced the self-renewal capacity of MS in vitro. A Wnt pathway reporter, TOP-eGFP lentivirus, was used to demonstrate the importance of the Wnt signaling pathway in the function of TICs. Consistent with our previous observation that $CD29^{H}CD24^{H}$ cells are enriched for functional TICs, TOP-eGFP positive cells are primarily $CD29^{H}CD24^{H}$. In vivo limiting dilution experiments with the eGFP-positive cells also validated the functional TIC activity of the cells with activation of the canonical Wnt pathway. The Akt inhibitor perifosine significantly reduced the proportion of TOP-eGFP-expressing cells (Fig. S4*C*). Perturbations of these pathways radiosensitized the TICs as demonstrated by their reduced self-renewal ability determined in MS assays. Most importantly, results from the in vivo limiting dilution transplantation experiments on dissociated tumor cells after each treatment confirmed the selective inhibition of TIC frequency by perifosine. Compared with controls, perifosine plus IR treatment resulted in a 4-fold reduction of the TIC frequency, and this effect was correlated with sustained foci following DNA damage. Thus, our studies nicely complement those of Korkaya et al. 2009 (12) and also demonstrate additional mechanisms by which the inhibition of the Akt/Wnt/β-catenin pathway may be used in conjunction with conventional radiation and chemotherapy to target not only the majority of the tumor cells, but also the subpopulation of TICs. However, the radiosensation of the TICs by perifosine may not be due solely to the inhibition of Akt signaling, because perifosine also has reported inhibitory effects on the assembly of both mTOR/raptor and mTOR/rictor complexes (30). Studies are in progress to compare these results obtained with perifosine with a new generation of more selective Akt inhibitors.

The use of a transplantable, syngeneic breast cancer model has allowed us to perform limiting dilution transplantation studies to evaluate the functional TIC frequency in vivo pre- and posttreatment. Moreover, the use of the canonical Wnt/β-catenin pathway reporter provides a valuable method to isolate and even image TICs in vivo and should provide a complementary approach to the use of FACS and cell surface markers for the identification of TICs. This may also provide an advantage for high-throughput methods for using small molecule libraries, as well as shRNAs in synthetic lethal screens to identify novel drugs and potentially unique druggable targets in TICs. The development of a new generation of Akt and Wnt pathway inhibitors by pharma will provide an exciting opportunity to determine the efficacy of these inhibitors in improved preclinical models, such as the transplantable p53 model. Importantly, many breast cancer patients receive radiation therapy after surgery. By selectively sensitizing TICs, our results indicate that pretreatment with Akt inhibitors may be of therapeutic benefit.

Materials and Methods

Materials. β-Catenin^{Ser552} was a kind gift from L. Li (University of Kansas Medical Center, Kansas City, KS). Wnt reporter lentivirus, TOP-eGFP, was a kind gift from I. Weissman (Stanford University, Stanford, CA). Perifosine was provided by KERYX Biopharmaceuticals. All other antibodies were purchased from commercial sources as listed in *SI Materials and Methods*.

Table 3. Reduced TIC frequency following perifosine plus radiation treatment as shown by limiting dilution transplantation

Cells injected (T1 TOP-eGFP)	10,000	1,000	100	10	TIC frequency (95% CI)
Control	12/12	11/12	2/12	0/18	1/454 (1/844–1/244)
IR	6/6	6/6	5/6	2/6	1/44 (1/109–1/18)*
Perifosine	6/6	3/6	0/6	0/6	1/1,626 (1/4,601–1/574)**
Perifosine + IR	6/6	2/6	0/6	0/6	1/2,357 (1/6,365–1/872)*
Cells injected (T7)	10,000	1,000	100	10	TIC frequency (95% CI)
Control	18/18	16/18	3/18	0/24	1/491 (1/815–1/296)
IR	12/12	12/12	5/12	0/12	1/195 (1/405–1/94)**
Perifosine	6/6	4/6	0/6	0/6	1/1,087 (1/2,899–1/408)
Perifosine + IR	6/6	2/6	0/6	0/6	1/2,357 (1/6,365–1/872)*

Tumors from three of each nontreated (control), IR-treated, perifosine-treated, and perifosine plus IR-treated group were dissociated and combined. The designated number of cells from each group was transplanted into 3-week-old BALB/c mice.
*$P < 0.007$; **$P < 0.05$.

Preparation of Single Mammary Tumor Cells. All animal protocols were reviewed and approved by the Animal Protocol Review Committee at Baylor College of Medicine. P53 null mammary tumors were generated as described (14, 31).

Flow Cytometry. Cells were labeled with antibodies at a concentration of 10 million cells/mL under optimized conditions (1:200 for FITC-CD29 and 1:100 for Pacific Blue-CD29, PE-CD24) and were subjected to FACS analysis and sorting on BD Biosciences LSR II and BD four laser FACSAriaII (Becton, Dickinson). Data analysis was performed on FlowJo version 8.8.6 (Tree Star).

In Vitro MS Assay. In vitro culturing and dissociating of the MSs are described in ref. 14. MS medium contains DMEM/F12 with 20 ng/mL bFGF, 20 ng/mL EGF, B27, 100 μg/mL gentimycin, and antibiotic–antimycotic. Perifosine was added after dissociation of the primary MSs at a designated concentration.

Transplantation into the Cleared Fat Pad. Clearance of mammary epithelial cells and transplantation procedures were performed as previously described (32). Following FACS, the designated number of cells was washed once with PBS and transplanted into the cleared fat pads of 3-week-old female BALB/c mice (Harlan). Tumor formation was monitored daily 2 weeks after the transplantation. TIC frequency and the Poisson distribution analysis were generated using R software (R Foundation for Statistical Computing).

Immunohistochemistry. FACS sorted and cytospun cells were stained with the antibodies against γ-H2AX (1:250) and 53BP1 (1:100) as described in *SI Materials and Methods*.

qPCR Analysis. Total RNA was isolated from the sorted subpopulations on the basis of Lin, CD29, and CD24 expression, using the PicoPure RNA isolation kit (Arcturus). cDNA production and qPCR reactions were performed as described in *SI Materials and Methods*.

IR Treatment. A ^{137}Cs irradiator, Unit GC-40 SN 192 (MDSNordion) was used to irradiate the mice at room temperature. A single dose of 6 Gy or 3 doses of 2 Gy every 16 h for 2 days were given.

Protein Extraction, SDS/PAGE, and Western Blot. Proteins were collected from FACS sorted TICs and non-TICs and from MSs and cells cultured on plastic from the dissociated p53 tumors, using the RIPA lysis and extraction buffer supplemented with the phosphatase inhibitor PhosSTOP (Roche) according to the manufacturer's recommendation. SDS/PAGE gradient gels (4–12%) were used (details in *SI Materials and Methods*).

Lentiviral Transduction. Single p53 null tumor cells (20,000/ well) were suspended into 24-well ultralow attachment plates and were transduced with lentivirus expressing either TOP-eGFP or the FOP-eGFP control at an optimized multiplicity of infection (MOI) of 5, respectively, for 16 h in a final volume of 0.8 mL serum-free MS medium. Transduced cells were washed in HBSS^{+} medium, before transplantation.

Drug Treatment. To get a sufficient number of tumor-bearing mice required for these studies, tumors were generated by transplantation of tumor fragments into the cleared fat pads of 3-week-old BALB/c mice as described previously (14). Treatment was started when the tumors were ≈5 mm in diameter and ended at the designated time point for each treatment group. Ten mice were given PBS in the control group with no perifosine; 5 mice from the above control group were irradiated with a single dose of 6 Gy at day 10, and tumors were analyzed 48 h later; 10 mice also were treated daily with perifosine (25 mg/kg by oral gavage according to manufacturer's recommendation) alone; and finally, 10 mice were treated daily with perifosine for 10 days as described above and were given a single dose of 6 Gy irradiation, and tumors again were analyzed 48 h later. Statistical differences for the tumor growths were determined using Student's *t* test. At the end of the treatment (right after the 10-day perifosine treatment or 2 days after the 10-day perifosine plus IR treatment), all mice were euthanized. Tumors were taken out for FACS analysis on the basis of cell surface marker expression (CD29 and CD24 or GFP) to determine the percentage of change of the TICs and non-TICs.

ACKNOWLEDGMENTS. We thank Dr. L. Li and Dr. I. Weissman for providing the antibody against β-catenin^{Ser552} and the Wnt signaling pathway reporter, TOP-eGFP or FOP-eGFP. We also thank Drs. W. Woodward, D. Medina, J. Herschkowitz, and H. LaMarca for constructive criticisms on this manuscript and Dr. S. Hilsenbeck for the advice on statistical analysis. These studies were supported by Grants CA16303 and U01-CA84243 from the National Institutes of Health (to J.M.R.) and by the Baylor College of Medicine Cytometry and Cell Sorting Core with funding from the National Institutes of Health (National Cancer Institute P30CA125123).

1. Rosen JM, Jordan CT (2009) The increasing complexity of the cancer stem cell paradigm. *Science* 324:1670–1673.
2. Li X, et al. (2008) Intrinsic resistance of tumorigenic breast cancer cells to chemotherapy. *J Natl Cancer Inst* 100:672–679.
3. Veeck J, et al. (2008) Wnt signalling in human breast cancer: Expression of the putative Wnt inhibitor Dickkopf-3 (DKK3) is frequently suppressed by promoter hypermethylation in mammary tumours. *Breast Cancer Res* 10:R82.
4. Watson SA (2001) Oncogenic targets of beta-catenin-mediated transcription in molecular pathogenesis of intestinal polyposis. *Lancet* 357:572–573.
5. Reya T, et al. (2003) A role for Wnt signalling in self-renewal of haematopoietic stem cells. *Nature* 423:409–414.
6. Groszer M, et al. (2006) PTEN negatively regulates neural stem cell self-renewal by modulating G0-G1 cell cycle entry. *Proc Natl Acad Sci USA* 103:111–116.
7. Zhang J, et al. (2006) PTEN maintains haematopoietic stem cells and acts in lineage choice and leukaemia prevention. *Nature* 441:518–522.
8. Pérez-Tenorio G, Stål O, Southeast Sweden Breast Cancer Group (2002) Activation of AKT/PKB in breast cancer predicts a worse outcome among endocrine treated patients. *Br J Cancer* 86:540–545.
9. Sos ML, et al. (2009) PTEN loss contributes to erlotinib resistance in EGFR-mutant lung cancer by activation of Akt and EGFR. *Cancer Res* 69:3256–3261.
10. Nagata Y, et al. (2004) PTEN activation contributes to tumor inhibition by trastuzumab, and loss of PTEN predicts trastuzumab resistance in patients. *Cancer Cell* 6:117–127.
11. Wang S, et al. (2006) Pten deletion leads to the expansion of a prostatic stem/progenitor cell subpopulation and tumor initiation. *Proc Natl Acad Sci USA* 103:1480–1485.
12. Korkaya H, et al. (2009) Regulation of mammary stem/progenitor cells by PTEN/Akt/beta-catenin signaling. *PLoS Biol* 7:e1000121.
13. Bleau AM, et al. (2009) PTEN/PI3K/Akt pathway regulates the side population phenotype and ABCG2 activity in glioma tumor stem-like cells. *Cell Stem Cell* 4:226–235.
14. Zhang M, et al. (2008) Identification of tumor-initiating cells in a p53-null mouse model of breast cancer. *Cancer Res* 68:4674–4682.
15. Shackleton M, et al. (2006) Generation of a functional mammary gland from a single stem cell. *Nature* 439:84–88.
16. Kelly PN, Dakic A, Adams JM, Nutt SL, Strasser A (2007) Tumor growth need not be driven by rare cancer stem cells. *Science* 317:337.
17. Fernandez-Capetillo O, et al. (2002) DNA damage-induced G2-M checkpoint activation by histone H2AX and 53BP1. *Nat Cell Biol* 4:993–997.
18. Diehn M, et al. (2009) Association of reactive oxygen species levels and radioresistance in cancer stem cells. *Nature* 458:780–783.
19. Kao GD, Jiang Z, Fernandes AM, Gupta AK, Maity A (2007) Inhibition of phosphatidylinositol-3-OH kinase/Akt signaling impairs DNA repair in glioblastoma cells following ionizing radiation. *J Biol Chem* 282:21206–21212.
20. He XC, et al. (2007) PTEN-deficient intestinal stem cells initiate intestinal polyposis. *Nat Genet* 39:189–198.
21. Nusse R, et al. (2008) Wnt signaling and stem cell control. *Cold Spring Harbor Symp Quant Biol* 73:59–66.
22. Woodward WA, et al. (2007) WNT/beta-catenin mediates radiation resistance of mouse mammary progenitor cells. *Proc Natl Acad Sci USA* 104:618–623.
23. Debeb BG, Xu W, Woodward WA (2009) Radiation resistance of breast cancer stem cells: Understanding the clinical framework. *J Mammary Gland Biol Neoplasia* 14:11–17.
24. Chen MS, et al. (2007) Wnt/beta-catenin mediates radiation resistance of Sca1+ progenitors in an immortalized mammary gland cell line. *J Cell Sci* 120:468–477.
25. Bao S, et al. (2006) Glioma stem cells promote radioresistance by preferential activation of the DNA damage response. *Nature* 444:756–760.
26. Gupta AK, et al. (2003) Radiation sensitization of human cancer cells in vivo by inhibiting the activity of PI3K using LY294002. *Int J Radiat Oncol Biol Phys* 56:846–853.
27. Jiang Z, et al. (2007) Phosphatase and tensin homologue deficiency in glioblastoma confers resistance to radiation and temozolomide that is reversed by the protease inhibitor nelfinavir. *Cancer Res* 67:4467–4473.
28. de la Peña L, et al. (2006) Inhibition of Akt by the alkylphospholipid perifosine does not enhance the radiosensitivity of human glioma cells. *Mol Cancer Ther* 5:1504–1510.
29. Li HF, Kim JS, Waldman T (2009) Radiation-induced Akt activation modulates radioresistance in human glioblastoma cells. *Radiat Oncol* 4:43.
30. Fu L, et al. (2009) Perifosine inhibits mammalian target of rapamycin signaling through facilitating degradation of major components in the mTOR axis and induces autophagy. *Cancer Res* 69:8967–8976.
31. Jerry DJ, et al. (2000) A mammary-specific model demonstrates the role of the p53 tumor suppressor gene in tumor development. *Oncogene* 19:1052–1058.
32. Medina D (1996) The mammary gland: A unique organ for the study of development and tumorigenesis. *J Mammary Gland Biol Neoplasia* 1:5–19.